Available online at www.sciencedirect.com
ScienceDirect
Journal of Molecular Structure 840 (2007) 71–89
Journal of MOLECULAR STRUCTURE
www.elsevier.com/locate/molstruc

Some polyhydroxy azo–azomethine derivatives of salicylaldehyde: Synthesis, characterization, spectroscopic, molecular structure and antimicrobial activity studies

Mustafa Odabaşoğlu [a,*], Çiğdem Albayrak [a], Reşit Özkanca [b], Fatma Zehra Aykan [b], Peter Lonecke [c]

[a] Department of Chemistry, Faculty of Arts and Sciences, Ondokuz Mayıs University, 55139 Kurupelit – Samsun, Turkey
[b] Department of Biology, Faculty of Arts and Sciences, Ondokuz Mayıs University, 55139 Kurupelit – Samsun, Turkey
[c] Universitat Leipzig Facultät für Chemie und Mineralogie, Leipzig, Germany

Received 9 September 2006; received in revised form 6 November 2006; accepted 10 November 2006
Available online 27 December 2006

Abstract

Some new substituted polyhydroxy azo–azomethine compounds were prepared by reaction of tris(hydroxymethyl)aminomethane with (*E*)-2-hydroxy-5-(phenyldiazenyl) benzaldehyde and its substituted derivatives. The structures of azo and azo–azomethine compounds were determined by IR, UV–vis, ^{1}H NMR and ^{13}C NMR spectroscopic techniques, and/or X-ray diffraction studies. According to IR spectra, all azo–azomethine compounds adopt keto form in solid state. UV–vis analysis has shown the presence of keto–enol tautomerism in solution for all azo–azomethine compounds, except that for nitro substituted derivative, enol form is dominantly favored in solution. At the same time, above mentioned derivative compounds were studied in vitro for their antimicrobial properties. Among the phenylazosalicylaldehyde series compound tested, 4-phenylazosalicylaldehyde, 4-(3-chlorophenylazo)salicylaldehyde, 4-(2-chlorophenylazo)salicylaldehyde, 4-(4-fluorophenylazo)salicylaldehyde, 4-(3-chlorophenylazo)salicylaldehyde and 4-(4-ethylphenylazo)salicylaldehyde showed a weak antimicrobial activity only against gram positive bacteria. On the contrary, phenylazosalicylaldehyde series compounds were reacted tris(hydroxmethyl)aminomethane, that exhibited a strong antimicrobial activity against gram positive bacteria, yeast and mould. Moreover, while the 2-{[1,3-dihydroxy-2-(hydroxymethyl)propan-2-ylimino]methyl}phenol did not show an inhibition on tested microorganism, the addition of phenyldiazine groups to 2-{[1,3-dihydroxy-2-(hydroxymethyl)propan-2-ylimino]methyl}phenol resulted in a strong increases in antimicrobial activity.

Keywords: Azo–azomethine compounds; Azo dyes; X-ray; UV–vis; IR; NMR; Tautomerism

1. Introduction

Azo compounds are the oldest and largest class of industrial synthesized organic dyes due to their versatile application in various fields, such as dyeing textile fiber, biomedical studies, advanced application in organic synthesis and high technology areas such as laser, liquid crystalline displays, electro-optical devices and ink-jet printers [1–3]. There are about 3000 azo dyes currently in use all over the world. The great majority of them are monoazo compounds, which have the common structure unit of the azo chromophore, —N=N—, linking two aromatic systems. The textile industry is the largest consumer of dyestuffs. Although some azo dyes have been reported to be toxic, dozens of additional monoazo dyes are permitted in drugs and cosmetics [4]. The pharmaceutical importance of compounds including an arylazo group has been extensively reported in the literature [5,6]. The oxidation–reduction behaviors of these compounds play an important role in its biological activity [7].

* Corresponding author. Tel.: +90 362 457 6020x5196; fax: +90 362 457 6081.
E-mail address: muodabas@omu.edu.tr (M. Odabaşoğlu).

0022-2860/$ - see front matter © 2006 Elsevier B.V. All rights reserved.
doi:10.1016/j.molstruc.2006.11.025

There is considerable interest in Schiff base ligands and their complexes due to their antitumor activities [8]. Azomethine derivatives are widely applied in biological systems and dyes [8,9]. In recent years, organic materials with second-order nonlinear optical properties have been extensively studied for use in photonic devices, such as high

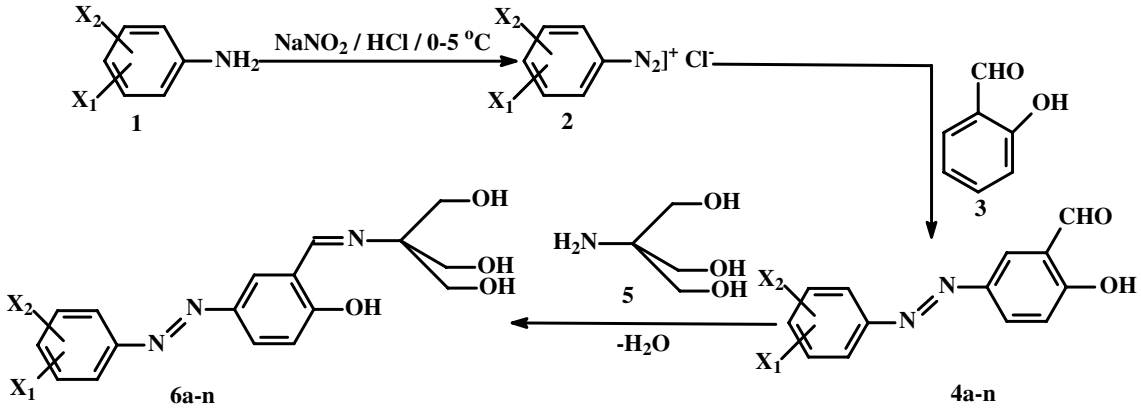

	X_1	X_2		X_1	X_2
a	H	H	**h**	4-I	H
b	2-Me	H	**i**	4-Me	H
c	2-Cl	H	**j**	4-Et	H
d	3-Cl	H	**k**	4-Bu^n	H
e	4-F	H	**l**	4-NO_2	H
f	4-Cl	H	**m**	4-Ac	H
g	4-Br	H	**n**	2-Cl	6-Cl

Scheme 1.

Table 1
Properties of 5-phenyldiazenylsalicylaldehydes **4** and their polyhydroxy azo–azomethine derivatives **6**

Compound	Yield (%)	Mp (°C)	% C		% H		% N	
			Calculated	Found	Calculated	Found	Calculated	Found
4a	96	128–130	–	–	–	–	–	–
6a	88	169–172	62.01	61.95	5.78	5.85	12.77	12.58
4b	82	113–115	–	–	–	–	–	–
6b	79	191–193	–	–	–	–	–	–
4c	85	151–153	–	–	–	–	–	–
6c	72	206–209	56.13	56.38	4.99	5.03	11.55	11.76
4d	91	139–141	–	–	–	–	–	–
6d	79	182–184	56.13	56.45	4.99	5.03	11.55	11.73
4e	87	168–171	–	–	–	–	–	–
6e	85	200–202	58.79	58.33	5.19	5.05	12.10	11.46
4f	83	211–213	–	–	–	–	–	–
6f	87	241–243	56.13	55.80	4.99	4.94	11.55	11.17
4g	74	216–218	–	–	–	–	–	–
6g	87	252–254	50.02	49.53	4.44	3.87	10.29	9.80
4h	85	219–223	–	–	–	–	–	–
6h	85	227–229	44.85	44.53	3.99	3.98	9.23	8.37
4i	80	151–154	–	–	–	–	–	–
6i	86	212–214	62.97	62.23	6.12	6.17	12.24	11.90
4j	90	123–126	–	–	–	–	–	–
6j	85	190–193	63.85	64.37	6.49	6.62	11.76	11.89
4k	89	96–98	–	–	–	–	–	–
6k	85	182–184	65.44	64.95	7.06	7.01	10.90	10.53
4l	87	195–198	–	–	–	–	–	–
6l	84	266–268	54.54	54.16	4.85	4.35	14.97	13.55
4m	70	176–179	–	–	–	–	–	–
6m	82	233–235	61.45	59.96	5.66	5.37	11.32	10.64
4n	65	165–167	–	–	–	–	–	–
6n	48	156–158	–	–	–	–	–	–

Table 2
UV–vis absorption bands of 5-phenyldiazenylsalicylaldehydes **4** and their polyhydroxy azo–azomethine derivatives **6** in DMSO

Compound	$\pi \rightarrow \pi^*$ nm (ε) (ε l mol^{-1} cm^{-1})	$\pi \rightarrow \pi^*$ nm (ε l mol^{-1} cm^{-1})	Compound	$\pi \rightarrow \pi^*$ nm (ε) (ε l mol^{-1} cm^{-1})	$\pi \rightarrow \pi^*$ nm (ε) (ε l mol^{-1} cm^{-1})
4a	341 (36300)	–	**4h**	355 (36850)	–
6a	361 (24800)	426 (13250)	**6h**	372 (31500)	426 (18400)
4b	372(20800)	–	**4i**	346 (39650)	–
6b	396(43100)	426(34800)	**6i**	366 (27300)	426 (14000)
4c	348 (28600)	–	**4j**	347 (39250)	–
6c	390 (24000)	426 (20550)	**6j**	366 (30600)	426 (15200)
4d	346 (31400)	–	**4k**	347 (38000)	–
6d	379 (25200)	426 (19900)	**6k**	366 (26850)	426 (13200)
4e	343 (27750)	–	**4l**	376 (33700)	–
6e	370 (24250)	426 (16000)	**6l**	423 (26150)	469 (28900)
4f	348 (44650)	–	**4m**	358 (37600)	–
6f	377 (25600)	426 (17550)	**6m**	382 (25200)	432 (19300)
4g	350 (36250)	–	**4n**	331(26200)	–
6g	369 (26300)	426 (16000)	**6n**	375(23700)	416(18900)

speed photonic switching, electro-optic modulators, components of optical communication systems and others [10–13]. *o*-Hydroxy Schiff bases exist as enol [14], keto [15–20] or enol/keto mixtures [21]. *N*-Substituted *o*-hydroxylimines have been reported to display thermochromism and photochromism in the solid state by H-atom transfer from the hydroxyl O-atom to the N-atom [17,18]. The proton tautomerism plays an important role in many fields of chemistry and especially biochemistry. Which tautomeric structure is dominant under certain conditions is important in terms of coloristic and technological properties of dyes [12]. Azo–azomethines have been extensively used as dyestuffs for wool, leather and synthetic fabrics because of their extraordinary coloring properties and in photonic devices, electrooptic modulators, components of optical communication systems of their second-order nonlinear optical properties [13,21–23].

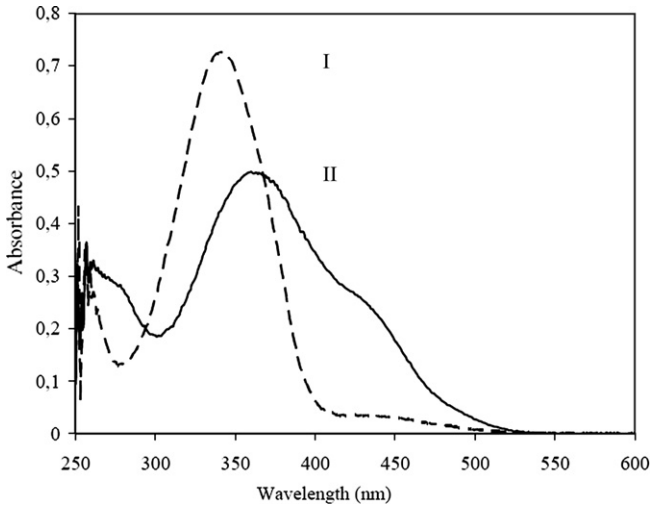

Fig. 1. Electronic spectra of **4a** (**I**) and **6a** (**II**) in DMSO.

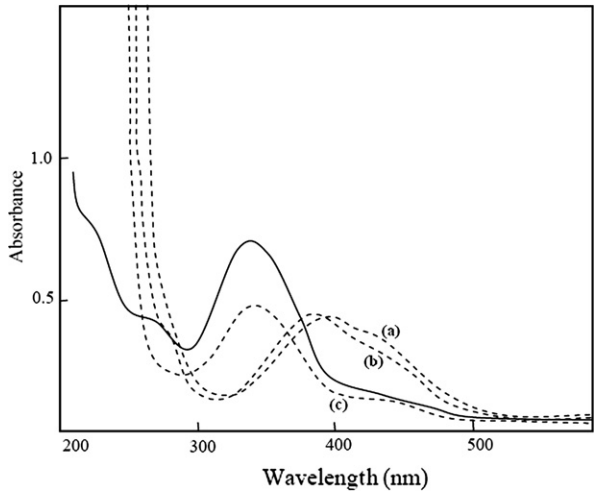

Fig. 2. Absorption spectra of **6a** in ethanol $C = 3.2 \times 10^{-5}$ M (———) and in DMF, $C = 1.6 \times 10^{-5}$ M (---------): (a) 0%; (b) 45% and (c) 60% water.

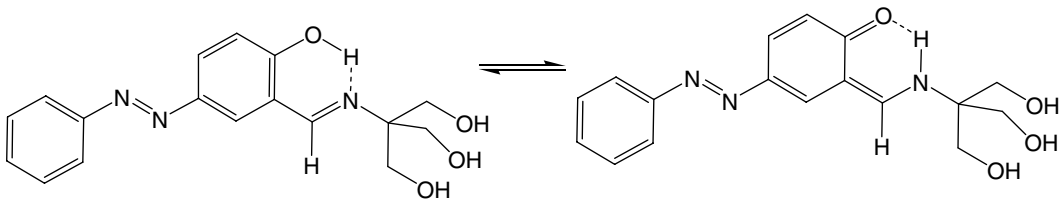

Scheme 2.

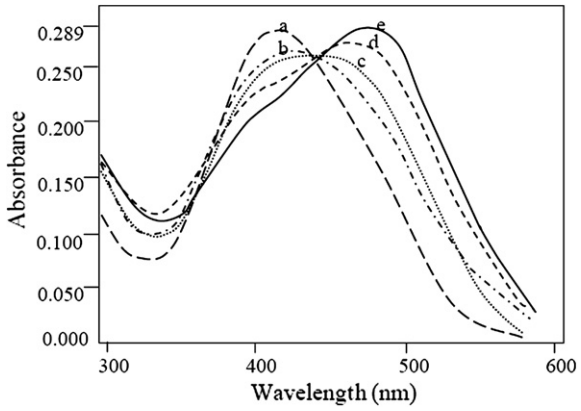

Fig. 3. Dependence of electronic absorption spectra of **6l** on temperature in EtOH: (a) −15 °C, (b) 50 °C, (c) 60 °C, (d) 68 °C, (e) 70 °C.

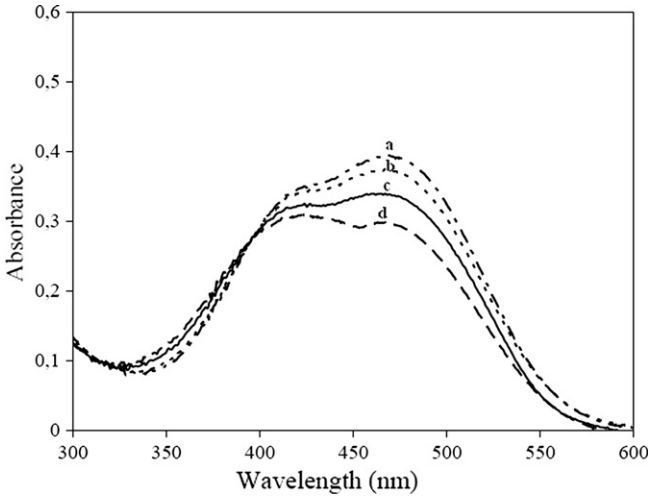

Fig. 4. Dependence of electronic absorption spectra of **6l** on temperature in DMSO: (a) 30 °C, (b) 50 °C, (c) 70 °C, (d) 80 °C.

Our interest has been focused on preparation of some polyhydroxy azo–azomethine derivatives with donor and acceptor groups, and investigation of their spectroscopic properties, molecular structure and antimicrobial activities.

2. Results and discussion

2.1. Synthesis

For synthesis of polyhydroxy azo–azomethine derivatives **6**, substituted anilines **1** were first diazotized using sodium nitrite in the presence of hydrochloric acid, which coupled with salicylaldehyde **3** to afford 5-phenyldiazenylsalicylaldehyde dyes **4** in good yields (Scheme 1 and Table 1). 5-Phenyldiazenylsalicylaldehydes **4** were purified by recrystallization from suitable solvents. The reaction of **4** with tris(hydroxymethyl)aminomethane (**5**) then afforded polyhydroxy azo–azomethine derivatives **6**, which were purified by recrystallization from suitable solvents and their purity was analyzed by thin-layer chromatography (Scheme 1 and Table 1).

2.2. UV–vis absorption spectra

Typical characteristic UV–vis absorption bands of 5-phenyldiazenylsalicylaldehydes **4** and their polyhydroxy azo–azomethine derivatives **6** in DMSO are given in Table 2.

The difference between UV–vis spectra of azo and azo–azomethine compounds is that $\pi \rightarrow \pi^*$ for azo group of azo–azomethine compounds is more red shifted than related azo compounds. This shift can be explained on the basis of the intramolecular hydrogen bonding between C=N and OH groups, which leaves a higher negative charge density on the oxygen atom of OH group. Another difference is $\pi \rightarrow \pi^*$ for keto form of azo–azomethine compounds since hydrogen is transferred from phenol group to imine nitrogen. Typical characteristic UV–vis absorption spectrum in DMSO for 5-phenyldiazenylsalicylaldehydes **4a** and their polyhydroxy azo–azomethine derivatives **6a** are given in Fig. 1.

The electronic spectra of **6a** were recorded in both DMF and EtOH between 200 and 600 nm (Fig. 2). These solvents were selected in order to obtain a difference in the position of tautomeric equilibrium (keto-amine ↔ enol-imine) (Scheme 2). The λ_{max} values of **6a** in DMF and EtOH are 393 (with shoulder at about 430 nm) and 339 nm, respectively. This tautomeric shift may be inferred from (i) selective solvation and (ii) the ability of the solvent to form stronger intermolecular H-bonds with a particular tautomeric form [24]. The absorption spectra of **6a** at different volume ratios of the applied pair of solvents DMF/water were also recorded. It was observed that the absorption of the band at 393 nm (probably enol-imine form) increased and shifted to 340 nm, while that of the other form (keto-amine at 340 nm) decreased with increasing of the volume content

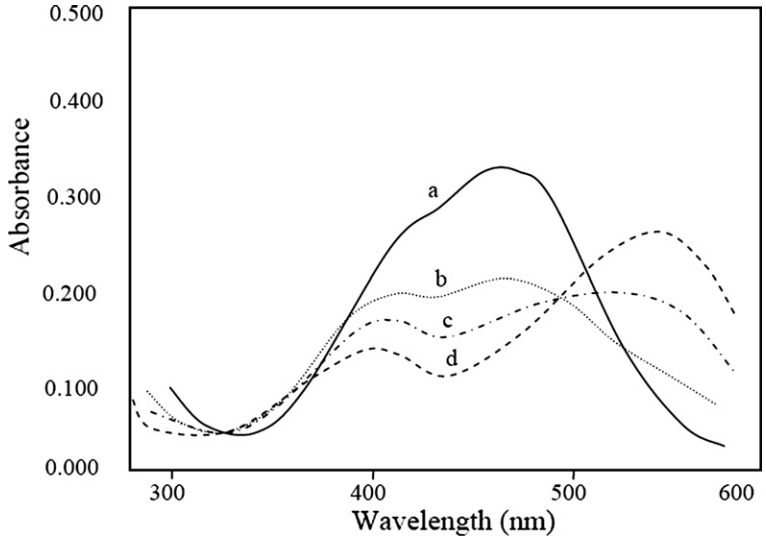

Fig. 5. Dependence of electronic absorption spectra of **6l** on temperature in DMF: (a) −10 °C, (b) 90 °C, (c) 96 °C, (d) 98 °C.

Table 3
Characteristic IR absorption bands of 5-phenyldiazenylsalicylaldehydes **4** and their polyhydroxy azo–azomethine derivatives **6**

Compound	OH (cm^{-1})	NHO (cm^{-1})	N=N (cm^{-1})	C=O (cm^{-1})	C—O$_{(Aliphatic)}$ (cm^{-1})	C—O$_{(Aromatic)}$ (cm^{-1})
4a	3224	–	1425	1668	–	1170–1150
6a	–	**3100–3400**	**1425**	**1635**	**1053**	–
4b	3421	–	1420	1654	–	1170–1150
6b	–	**3100–3400**	**1419**	**1645**	**1056**	–
4c	3200	–	1420	1670	–	1170–1150
6c	–	**3100–3400**	**1425**	**1651**	**1055**	–
4d	3213	–	1411	1662	–	1170–1150
6d	–	**3100–3400**	**1413**	**1639**	**1051**	–
4e	3263	–	1409	1670	–	1170–1150
6e	–	**3100–3400**	**1431**	**1645**	**1045**	–
4f	3200	–	1425	1670	–	1170–1150
6f	–	**3100–3400**	**1427**	**1647**	**1059**	–
4g	3200	–	1424	1668	–	1170–1150
6g		**3100–3400**	**1425**	**1645**	**1062**	–
4h	3200	–	1425	1668	–	1170–1150
6h	–	**3100–3400**	**1425**	**1643**	**1058**	–
4i	3200	–	1422	1655	–	1170–1150
6i	–	**3100–3400**	**1423**	**1660**	**1064**	–
4j	3200	–	1423	1651	–	1170–1150
6j	–	**3100–3400**	**1425**	**1658**	**1062**	–
4k	3200	–	1412	1666	–	1170–1150
6k	–	**3100–3400**	**1423**	**1660**	**1062**	–
4l	3200	–	1420	1655	–	1170–1150
6l		**3100–3400**	**1419**	**1651**	**1058**	–
4m	3200	–	1413	1678 1662	–	1170–1150
6m	–	**3100–3400**	**1421**	**1670** **1643**	**1058**	–
4n	3200		1421	1624	–	1186
6n	–	**3100–3400**	**1421**	**1639**	**1047**	–

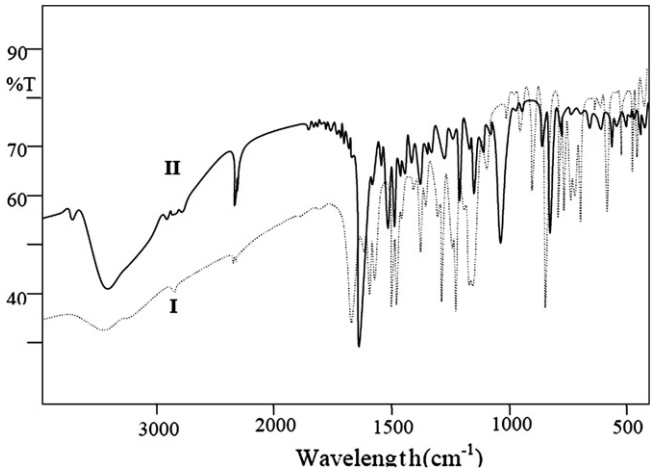

Fig. 6. IR spectra of **4e** (I) and **6e** (II).

of water (Fig. 2). H_2O leads to an increase of the H form [24].

The UV–vis spectra of compounds **6l** were studied at different temperature in EtOH. Fig. 3 shows the UV spectra of compound **6l** at different temperatures. The compound **6l** shows two absorptions at room temperature in the range of 300–600 nm. One is 393 nm for enol-imine form while other is 453 nm for keto-amine form. When the solution of compound **6l** was cooled at −15 °C, the color of solution was turned from orange to yellow and the absorption band (453 nm) for keto form was disappeared at the UV–vis spectra. When the cold solution was heated, the absorption band for keto form was appeared again. This implies that there is enol–keto equilibrium and this equilibrium depends on temperature. Phenol–imine tautomer is dominant at low temperature in EtOH, while keto-amine tautomer is dominant at high temperature. The phenol–imine tautomerism in the spectrum of **6m** is dominant as in the spectrum of **6l** in ethyl alcohol at low temperature, but there is no significant changes at the equilibrium of other azo–azomethines.

Table 4
^{1}H NMR signals of 5-phenyldiazenylsalicylaldehydes **4**

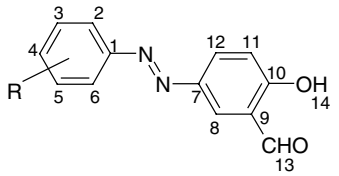

	4a	4b	4c	4d	4e	4f	4g	4h	4i	4j	4k	4l	4m	4n
H2	7.85063 (dd), $J_{2,3} = 8.032$, $J_{2,4} = 1.98$	–	–	7.82769 (t), $J_{2,6} = 2.152$, $J_{2,4} = 2.152$	7.9201 (dd), $J_{2,3} = 8.81$, $J_{HF} = 5.27$	7.63014 (d), $J_{2,3} = 8.76$	7.7791	7.62033 (d), $J_{2,3} = 8.262$	7.73889 (d), $J_{2,3} = 8.17$	7.75946 (d), $J_{2,3} = 8.17$	7.72988 (d), $J_{2,3} = 8.20$	7.98545 (d), $J_{2,3} = 9.016$	7.90989 (d), $J_{2,3} = 8.238$	–
H3	7.57259 (t), $J_{3,2} = 8.032$, $J_{3,4} = 8.032$	7.43714 (d), $J_{3,4} = 7.56$	7.6450 (dd), $J_{3,4} = 7.62$, $J_{3,5} = 2.1$	–	7.4043 (dd), $J_{3,2} = 8.81$, $J_{HF} = 8.81$	7.86931 (d), $J_{3,2} = 8.76$	7.7791	7.93655 (d), $J_{3,2} = 8.262$	7.34364 (d), $J_{3,2} = 8.17$	7.36687 (d), $J_{3,2} = 8.17$	7.30735 (d), $J_{3,2} = 8.20$	8.36811 (d), $J_{3,2} = 9.016$	8.15725 (d), $J_{3,2} = 8.238$	7.5972 (d), $J_{3,4} = 7.826$
H4	7.55635 (tt), $J_{4,3} = 8.032$, $J_{4,5} = 8.032$, $J_{4,2} = 1.98$, $J_{4,6} = 1.98$	7.27547 (t), $J_{4,3} = 7.56$, $J_{4,5} = 7.56$	7.45885 (td), $J_{4,3} = 7.62$, $J_{4,5} = 7.62$, $J_{4,6} = 1.68$	7.58851 (dt), $J_{4,5} = 7.562$, $J_{4,2} = 2.152$, $J_{4,6} = 2.152$	–	–	–	–	–	–	–	–	–	7.3763 (t), $J_{4,3} = 7.826$, $J_{4,5} = 7.826$
H5	7.57259 (t), $J_{5,6} = 8.032$, $J_{5,4} = 8.032$	7.34588 (t), $J_{5,6} = 7.56$, $J_{5,4} = 7.56$	7.52832 (td), $J_{5,6} = 7.72$, $J_{5,4} = 7.62$, $J_{5,3} = 2.1$	7.61980 (t), $J_{5,6} = 7.562$, $J_{5,4} = 7.562$	7.4043 (dd), $J_{5,6} = 8.81$, $J_{HF} = 8.81$	7.86931 (d), $J_{3,2} = 8.76$	7.7791	7.93655 (d), $J_{3,2} = 8.262$	7.34364 (d), $J_{3,2} = 8.17$	7.36687 (d), $J_{3,2} = 8.17$	7.30735 (d), $J_{3,2} = 8.20$	8.36811 (d), $J_{3,2} = 9.016$	8.15725 (d), $J_{3,2} = 8.238$	7.5972 (d), $J_{5,4} = 7.826$
H6	7.8563 (dd), $J_{6,5} = 8.032$, $J_{6,4} = 1.98$	7.54181 (d), $J_{6,5} = 7.56$	7.68734 (dd), $J_{6,5} = 7.72$, $J_{6,4} = 1.68$	7.8388 (dt), $J_{6,5} = 7.152$, $J_{6,4} = 2.152$, $J_{6,2} = 2.152$	7.9201 (dd), $J_{6,5} = 8.81$, $J_{HF} = 5.27$	7.63014 (d), $J_{2,3} = 8.76$	7.7791	7.62033 (d), $J_{2,3} = 8.262$	7.73889 (d), $J_{2,3} = 8.17$	7.75946 (d), $J_{2,3} = 8.17$	7.72988 (d), $J_{2,3} = 8.20$	7.98545 (d), $J_{2,3} = 9.016$	7.90989 (d), $J_{2,3} = 8.238$	–
H8	8.1726 (d), $J_{8,12} = 2.38$	8.16501 (d), $J_{8,12} = 2.504$	8.19225 (d), $J_{8,12} = 2.50$	8.18930 (d), $J_{8,12} = 2.50$	8.15715 (d), $J_{8,12} = 2.50$	8.17746 (d), $J_{8,12} = 2.54$	8.16715 (d), $J_{8,12} = 2.34$	8.16848 (d), $J_{8,12} = 2.52$	8.12684 (d), $J_{8,12} = 2.38$	8.14570 (d), $J_{8,12} = 2.242$	8.13349 (d), $J_{8,12} = 2.36$	8.17885 (d), $J_{8,12} = 2.522$	8.17981 (d), $J_{8,12} = 1.78$	8.1789 (d), $J_{8,12} = 2.51$
H11	7.1860 (d), $J_{11,12} = 8.84$	7.19261 (d), $J_{11,12} = 8.81$	7.2145 (d), $J_{11,12} = 8.85$	7.19125 (d), $J_{11,12} = 8.84$	7.18432 (d), $J_{11,12} = 8.80$	7.18521 (d), $J_{11,12} = 8.83$	7.1697 (d), $J_{11,12} = 8.4$	7.17759 (d), $J_{11,12} = 8.886$	7.16167 (d), $J_{11,12} = 8.77$	7.16900 (d), $J_{11,12} = 8.79$	7.15870 (d), $J_{11,12} = 8.84$	7.18925 (d), $J_{11,12} = 8.79$	7.18151 (d), $J_{11,12} = 8.70$	7.2219 (d), $J_{11,12} = 8.83$
H12	8.0792 (dd), $J_{12,11} = 8.84$, $J_{12,8} = 2.38$	8.07806 (dd), $J_{12,11} = 8.81$, $J_{12,8} = 2.504$	8.088 (dd), $J_{12,11} = 8.85$, $J_{12,8} = 2.50$	8.09522 (dd), $J_{12,11} = 8.84$, $J_{12,8} = 2.50$	8.06368 (dd), $J_{12,11} = 8.80$, $J_{12,8} = 2.50$	8.08278 (dd), $J_{12,11} = 8.83$, $J_{12,8} = 2.54$	8.08165 (dd), $J_{12,11} = 8.4$, $J_{12,8} = 2.34$	8.07582 (dd), $J_{12,11} = 8.86$, $J_{12,8} = 2.52$	8.03726 (dd), $J_{12,11} = 8.77$, $J_{12,8} = 2.38$	8.03984 (ddd), $J_{12,11} = 8.79$, $J_{12,8} = 2.242$, $J_{12,13} = 0.98$	8.02298 (ddd), $J_{12,11} = 8.84$, $J_{12,8} = 2.36$, $J_{12,13} = 0.58$	8.09124 (dd), $J_{12,11} = 8.79$, $J_{12,8} = 2.522$	Under H5	8.08768 (dd), $J_{12,11} = 8.83$, $J_{12,8} = 2.51$

H13	10.3611	10.3595	10.3610	10.3474	10.3549	10.3530	10.3352	10.3429	10.3402	10.3468, $J_{13,12} = 0.98$	10.3457 (d), $J_{13,12} = 0.58$	10.3321	10.3401	10.3468
H14	11.5254 (11.3189)*	11.5054 (11.3188)*	−(11.3702)*	−(11.3625)*	11.5420 (11.3143)*	−(11.3415)*	− (11.3443)*	−(11.3466)*	−(11.2908)*	−(11.2901)*	−(11.2892)*	−(11.4554)*	−(11.3873)*	10.34.68 (13.1304)*
$-CH_2$	−	−	−	−	−	−	−	−	−	−	2.58671 (t), $J_{15,16} = \sim 7.5$	−	−	−
$-CH_2$	−	−	−	−	−	−	−	−	−	−	1.52275 (p), $J_{16,15} = \sim 7.5$, $J_{16,17} = \sim 7.5$	−	−	−
$-CH_2$	−	−	−	−	−	−	−	−	−	2.66153 (q), $J_{15,16} = 7.6$	1.25595 (h), $J_{17,16} = \sim 7.5$, $J_{17,18} = \sim 7.5$	−	−	−
$-CH_3$	−	2.6459	−	−	−	−	−	−	2.3622	1,1939 (t), $J_{16,15} = 7.6$	0.84443 (t), $J_{18,17} = \sim 7.5$	−	−	−
$-COCH_3$	−		−	−	−	−	−	−	−	−	−	−	2.61549	−

* In $CDCl_3$.

The UV–vis spectra of compounds **6l** were studied at different temperature in DMSO, as well as illustrated in Fig. 4. Keto-amine tautomer is dominant at low temperature while phenol–imine form is dominant at high temperature. The UV–vis spectra of **6l** and **6m** showed a similar behaviour, in contrast, other azo–azomethines demonstrated very little changes in DMSO.

The UV–vis spectra of compounds **6l** were also studied at different temperature in DMF as shown in Fig. 5. Compound **6l** shows two absorptions at room temperature in the range of 300–600 nm; 422 nm for enol-imine form and 469 nm for keto-amine form. When the solution was heated, the new absorption band was appeared at 537 nm at 90 °C. This absorption band represents the charge transfer interaction between keto and enol molecules as observed for all azo–azomethine compounds (**6a**–**n**).

2.3. IR absorption spectra

The characteristic IR absorption bands of 5-phenyldiazenylsalicylaldehydes **4** and their polyhydroxy azo–azomethine derivatives **6** were determined in KBr disk. Table 3 shows typical characteristic IR absorption bands. The N—H···O bands are located at about the range 3100–3500 cm^{-1} in azo–azomethine compounds. Results from X-ray diffraction studies show very short C=O bonds, indicating their double bond characteristic. The peaks for azo–azomethine compounds are very sharp and at 1630–1670 cm^{-1}, which corresponds to ν(C=O) vibration, suggesting azo–azomethine compounds in the solid state exists as a keto-amine tautomer. Another evidence for existence of the keto-amine tautomer is that phenolic ν(C—O) vibration, which observed in the range 1170–1150 cm^{-1} in azo compounds, disappeared in azo–azomethine derivatives. Aliphatic ν(C—O) vibration is in the range 1050–1070 cm^{-1}. Fig. 6 shows the IR spectra of compound **4e** and **6e**.

2.4. NMR investigations

In their ^{1}H NMR spectra, all azo compounds **4** show a peak at 10.32–10.37 ppm, belonging to the aldehyde group. However, this aldehyde peaks disappear in azo–azomethine derivatives. CH—N proton appears in the range of 8.60–8.67 ppm (Table 4). ^{1}H NMR spectra of azo compounds show d peaks at 8.11–8.20 ppm, d at 7.14–7.22 ppm and dd at 8.01–8.1 ppm, which are attributed to phenyl group including aldehyde group. The corresponding peaks in ^{1}H NMR spectra of azo–azomethine compounds are d at 8.0–8.19 ppm, d at 6.58–6.67 ppm and dd at 7.85–7.91 ppm. These chemical shift differences clearly indicate that azo–azomethine compounds shift to keto structures. In the ^{1}H NMR spectrum of **6e** (Fig. 8), H13 and H14 protons split into doublets since the hydrogen (H14) of phenol group is transferred to the imine nitrogen and H13 proton interact with H14 proton ($J_{13,14} = 10.7$ Hz). In compounds

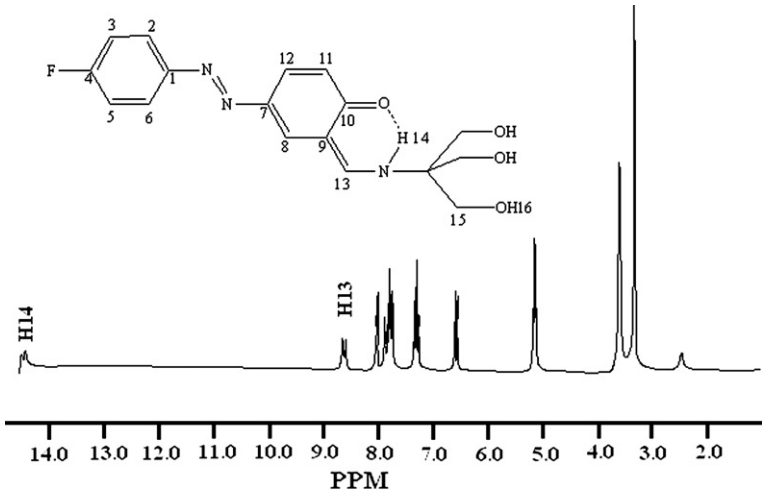

Fig. 7. ^{1}H NMR spectrum of **6e**.

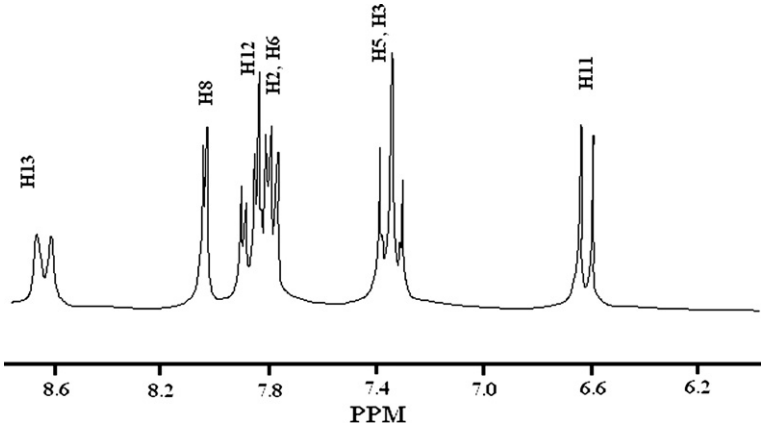

Fig. 8. ^{1}H NMR spectrum of **6e**.

6a, **6d**, **6l** and **6m**, similar doublets are observed, as well (Table 6). This shows that azo–azomethine compounds exist as keto-amine tautomers (Fig. 7).

In contrast to the other *p*-substituted azo and azo–azomethine compounds, in ^{1}H NMR spectra of **4e** and **6e**, since the F nucleus couples to H2, H6 and H3, H5 protons, they respectively are seen as a quartet and a triplet (Fig. 9). Coupling constants for proton–fluorine are different because the fluorine atom couples differently to the *ortho*-, *meta*- and *para*-protons. The triplet can be shown as a result of consecutive splitting of the H3, H5 absorption by the H2, H6 and F nucleus. The peaks overlap since the coupling constants are identical ($J_{HF} = J_{3,2} = 8.72$ Hz). The H2, H6 protons are coupled to both the H3, H5 protons and F nucleus and show doublet of doublets ($J_{2,3} = 8.72$ Hz, $J_{HF} = 5.34$ Hz). This result is in accordance with the literature [25]. The chemical shift values are shown in Table 6.

In the ^{1}H NMR spectrum of **6e** (Fig. 10), alcoholic O—H (H16) and adjacent –CH_2 (H15) protons interact with each other and H15 proton split into a doublet while H16 proton gives a triplet ($J_{15,16} = 5.18$) (Fig. 10). Similar situations were observed for compounds **6a**, **6c**, **6d**, **6f**, **6i**, **6k**, **6l** and **6m**, as well (Table 6).

Aldehydic carbons observed in azo compounds in the range 187.2–188 ppm disappear in azo–azomethine derivatives and CH—N carbons appear in the range of 164.4–165.3 ppm instead of aldehydic carbons. Despite phenolic carbons (C10) in ^{13}C NMR spectra of azo compounds appear at 162.8–164.5 ppm, the corresponding peaks are observed at 175.7–179.5 ppm in azo–azomethine derivatives, which prove that azo–azomethine compounds shift to keto structure. The chemical shifts of carbons for azo and azo–azomethine compounds are shown in Tables 5 and 7, respectively. ^{13}C NMR spectra of azo compounds show peaks at 129.1–130 ppm (C8), at 118.1–118.6 ppm (C11) and at 123.6–125 ppm (C12), which are attributed to phenyl group bearing aldehyde functionality. The corresponding peaks in ^{13}C NMR spectra of azo–azomethine compounds are at 132.2–138.5 ppm (C8), at 114.2–114.9 ppm (C11) and at 126.2–126.5 ppm (C12). These chemical shifts are supported by ^{1}H NMR spectra, as well. These results show that azo–azomethine compounds shift to keto structure. According to ^{13}C

Table 5
^{13}C NMR signals of 5-phenyldiazenylsalicylaldehydes **4**

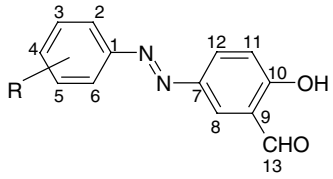

	4a	4b	4c	4d	4e	4f	4h	4i	4j	4k	4l	4m	4n
C1	151.804	149.831	147.831	152.872	148.530	150.426	151.209	149.958	150.152	150.077	155.163	154.212	147.246
C2	122.178	137.052	133.365	122.163	124.479 (d), $J_{C2F} = 9.1$	129.398	129.637	122.295	122.384	122.231	123.186	122.318	129.459
C3	129.213	130.811	130.542	134.102	116.186 (d), $J_{C3F} = 23.05$	123.861	138.288	129.832	128.613	129.014	123.186	129.402	128.060
C4	130.888	131.238	132.051	131.045	163.400 (d), $J_{C4F} = 251.6$	135.413	97.9717	141.221	147.351	145.351	148.129	137.999	141.076
C5	129.213	126.455	117.481	130.442	116.186 (d), $J_{C5F} = 23.05$	123.861	138.288	129.832	128.613	129.014	123.186	129.402	128.060
C6	122.178	115.070	127.908	120.759	124.479 (d), $J_{C6F} = 9.1$	129.398	129.637	122.295	122.384	122.231	123.186	122.318	129.459
C7	144.779	145.283	145.054	144.640	144.653	144.652	144.710	144.876	144.915	144.869	144.839	144.880	144.801
C8	129.469	129.288	129.666	129.741	129.487	129.584	129.637	129.523	129.500	129.363	129.929	129.755	129.459
C9	122.477	122.480	122.616	122.611	122.507	122.581	122.604	122.526	122.516	122.454	122.736	122.627	122.776
C10	163.086	163.023	163.673	163.637	163.150	163.418	163.429	162.965	162.965	162.910	164.266	163.709	164.483
C11	118.256	118.306	118.478	118.416	118.273	118.416	118.426	118.291	118.275	118.202	118.576	118.424	118.773
C12	123.864	124.203	124.499	124.436	123.898	124.006	124.097	123.721	123.809	123.749	124.929	124.421	124.845
C13	187.356	187.461	187.681	187.602	187.559	187.615	187.547	187.430	187.322	187.312	187.929	187.690	187.753
$-CH_2$	–	–	–	–	–	–	–	–	–	34.537	–	–	–
$-CH_2$	–	–	–	–	–	–	–	–	–	32.661	–	–	–
$-CH_2$	–	–	–	–	–	–	–	–	27.981	21.586	–	–	–
$-CH_3$	–	16.958	–	–	–	–	–	20.914	15.134	13.533	–	–	–
$COCH_3$	–	–	–	–	–	–	–	–	–	–	–	26.763	–
CO	–	–	–	–	–	–	–	–	–	–	–	180.999	–

NMR spectra, azo–azomethine compounds exist as keto-amine tautomers, as well. ^{13}C NMR spectrum of **6e** is shown in Fig. 11. As in the ^{1}H NMR spectra of **4e** and **6e**, the F nucleus couples to carbons of fluorine-containing aromatic ring and C1, C4 and C2, C6 and C3, C5 carbons give a doublet in the ^{13}C NMR spectra (Fig. 12). Coupling constants for carbon–fluorine are different as the fluorine atom couples differently to the *ipso*-, *ortho*-, *meta*- and *para*-carbons. Coupling constants for carbon–fluorine are given in Table 7. This result is in accordance with the literature [25]. The chemical shift values of 6 compounds are summarized in Table 7.

2.5. Description of the crystal structures

A summary of crystallographic data, experimental details, and refinement results for **4i** and **6a** are given in Table 8. Table 9 shows the selected bond distances and bond angles for **4i** and **6a**. SHELXS-97 [26] and SHELXL-97 [27] were used for the structure solution and refinement.

The molecular structure of compound **4i** is shown in Fig. 13 with the atom numbering scheme. The compound consists of two aromatic rings (C1–C6 and C7–C12), and an azo frame (C1–N1–N2–C7). In **4i**, the aromatic rings, which adopt a trans configuration about the N=N double bond, are nearly coplanar, with a dihedral angle of 8.10(7)° between them. Also, our previous X-ray investigation that the other phenyldiazenylsalicylaldehydes are nearly coplanar and the dihedral angles these compounds are as in Table 11[28–31]. The 4-methyl phenyldiazenylsalicylaldehyde molecules are linked into $[S(6)R_2^2(4)S(6)R_2^2(4)R_4^4(20)R_4^4(20)]$ motifs [32] (Fig. 14) and C—H···π interactions [C14—H14c···Cg1^{i} = 3.519(3)Å, H14c···Cg1 = 2.61(3)Å, C14—H14c···Cg1 = 153(2)°; Cg1 = C1–C6 ring, (i) = x, $1 + y, z$ (Fig. 15)]. A significant intramolecular interaction is noted, involving phenolic atom H and carbonyl atom

Table 6
^{1}H NMR signals of azo–azomethine compounds **6**

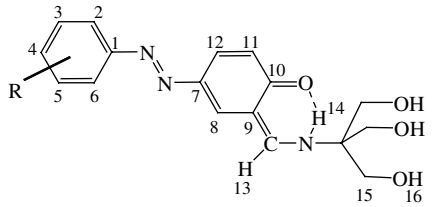

	6a	6b	6c	6d	6e	6f	6g	6h	6i	6j	6k	6l	6m	6n
H2	7.75332 (dd), $J_{2,3} = 7.54$, $J_{2,4} = 1.44$	–	–	7.71465 (t), $J_{2,6} = 1.42$, $J_{2,4} = 1.42$	7.8077 (dd), $J_{2,3} = 8.72$, $J_{HF} = 5.34$	7.55690 (d), $J_{2,3} = 8.708$	7.69296 (s)	7.52705 (d) $J_{2,3} = 8.552$	7.66197 (d) $J_{2,3} = 8.228$	7.69155 (d) $J_{2,3} = 8.24$	7.68004 (d) $J_{2,3} = 8.264$	7.90728 (d) $J_{3,2} = 8,98$	7.82124 (d) $J_{3,2} = 8.594$	–
H3	7.5267 (t), $J_{3,2} = 7.54$, $J_{3,4} = 7.54$	7.34955 (dd), $J_{3,4} = 6.67$, $J_{3,5} = 2.59$	7,602795 (dd), $J_{3,4} = 7.1$, $J_{3,5} = 1.076$	–	7.3507 (dd), $J_{3,2} = 8.72$, $J_{HF} = 8.72$	7.75141 (d), $J_{3,2} = 8.708$	7.69296 (s)	7.87341 (d), $J_{3,2} = 8.552$	7.31797 (d), $J_{3,2} = 8.228$	7.33348 (d), $J_{3,2} = 8.24$	7.32897 (d), $J_{3,2} = 8.264$	8.361945 (d), $J_{2,3} = 8.98$	8.084715 (d), $J_{2,3} = 8.594$	7.55736 (d), $J_{3,4} = 7.814$
H4	7.42140 (tt), $J_{4,3} = 7.54$, $J_{4,5} = 7.54$, $J_{4,2} = 1.44$, $J_{4,6} = 1.44$	7.25254 (td) $J_{4,3} = 6.67$, $J_{4,5} = 6.67$, $J_{4,6} = 2.59$	7.40762 (td), $J_{4,3} = 7.1$, $J_{4,5} = 7.1$, $J_{4,6} = 1.518$	7.475635 (dt), $J_{4,5} = 7.972$, $J_{4,2} = 1.42$, $J_{4,6} = 1.42$	–	–	–	–	–	–	–	–	–	7.3129 (t), $J_{4,3} = 7.814$, $J_{4,5} = 7.814$
H5	7.5267 (t), $J_{5,6} = 7.54$, $J_{5,4} = 7.54$	7.27486 (td), $J_{5,6} = 6.67$, $J_{5,4} = 6.67$, $J_{5,3} = 2.59$	7.422355 (td), $J_{5,6} = 7.1$, $J_{5,4} = 7.1$, $J_{5,3} = 1.076$	7.55974 (t), $J_{5,6} = 7.972$, $J_{5,4} = 7.972$	7.3507 (dd), $J_{5,6} = 8.72$, $J_{HF} = 8.72$	7.75141 (d), $J_{5,6} = 8.708$	7.69296 (s)	7.87341 (d), $J_{5,6} = 8.552$	7.31797, $J_{5,6} = 8.228$	7.33348 (d), $J_{5,6} = 8.24$	7.32897 (d), $J_{5,6} = 8.264$	8.361945 (d), $J_{2,3} = 8.98$	8.084715 (d), $J_{5,6} = 8.594$	7.55736 (d), $J_{5,4} = 7.814$
H6	7.8563 (dd), $J_{6,5} = 7.54$, $J_{6,4} = 1.44$	7.50970 (dd), $J_{6,5} = 6.67$, $J_{6,4} = 2.59$	7.61655 (dd), $J_{6,5} = 7.1$, $J_{6,4} = 1.518$	7.726305 (dt), $J_{6,5} = 7.972$, $J_{6,4} = 1.42$, $J_{6,2} = 1.42$	7.8077 (dd), $J_{6,5} = 8.72$, $J_{HF} = 5.34$	7.55690 (d), $J_{6,5} = 8.708$	7.69296 (s)	7.52705 (d), $J_{6,5} = 8.552$	7.66197 (d) $J_{6,5} = 8.228$	7.69155 (d), $J_{6,5} = 8.24$	7.68004 (d), $J_{6,5} = 8.264$	7.90728 (d), $J_{3,2} = 8.98$	7.82124 (d), $J_{6,5} = 8.594$	–
H8	8.05284 (d), $J_{8,12} = 2.656$	8.03852 (d), $J_{8,12} = 2.49$	8.088505 (d), $J_{8,12} = 2.646$	8.0938 (d), $J_{8,12} = 2.628$	8.04246 (d), $J_{8,12} = 2.622$	8.0369 (d), $J_{8,12} = 2.586$	8.05915 (d), $J_{8,12} = 2.54$	8.03934 (s)	8.012515 (d), $J_{8,12} = 2,59$	8.01839 (d), $J_{8,12} = 2,49$	8.00369 (d), $J_{8,12} = 2.484$	8.18761 (d), $J_{8,12} = 2.164$	8.13532 (d), $J_{8,12} = 2.612$	8.1012 (d), $J_{8,12} = 2.16$
H11	6.62586 (d), $J_{11,12} = 9.42$	6.66174 (d), $J_{11,12} = 9.36$	6.632205 (d), $J_{11,12} = 9.5$	6.60796 (d), $J_{11,12} = 9.52$	6.627535 (d), $J_{11,12} = 9.46$	6.62566 (d), $J_{11,12} = 9.50$	6.61395 (d), $J_{11,12} = 9.38$	6.622215 (d), $J_{11,12} = 9.52$	6.63157 (d), $J_{11,12} = 9,47$	6.6614 (d), $J_{11,12} = 9.35$	6.6468 (d), $J_{11,12} = 9.37$	6.59595 (d), $J_{11,12} = 9.61$	6.60399 (d), $J_{11,12} = 9.548$	6.56778 (d), $J_{11,12} = 9.58$
H12	7.88577 (dd), $J_{12,11} = 9.42$, $J_{12,8} = 2.656$	7.89718 (dd), $J_{12,11} = 9.36$, $J_{12,8} = 2.49$	7.89899 (dd), $J_{12,11} = 9.5$, $J_{12,8} = 2.646$	7.884235 (dd), $J_{12,11} = 9.52$, $J_{12,8} = 2.628$	7.874505 (dd), $J_{12,11} = 9.46$, $J_{12,8} = 2.622$	7.87254 (dd), $J_{12,11} = 9.50$, $J_{12,8} = 2.586$	7.87254 (dd), $J_{12,11} = 9.38$, $J_{12,8} = 2.54$	7.87341 (dd), $J_{12,11} = 9.52$	7,867565 (dd), $J_{12,11} = 9.47$, $J_{12,8} = 2.59$	7.883635 (dd), $J_{12,11} = 9.35$, $J_{12,8} = 2.49$	7,871015 (dd), $J_{12,11} = 9.37$, $J_{12,8} = 2.484$	7.90728 (dd), $J_{12,11} = 9.61$, $J_{12,8} = 2.164$	7.90985 (dd), $J_{12,11} = 9.548$, $J_{12,8} = 2.612$	7.84315 (dd), $J_{12,11} = 9.58$, $J_{12,8} = 2.16$

H13	8.63625 (d), $J_{13,14}=11.4$	8.64426 (s)	8.64356 (s)	8.62985 (d), $J_{13,14}=11.3$	8.63675 (d), $J_{13,14}=10.7$	8.61241 (s)	8.6168 (s)	8.6127 (s)	8.6115 (s)	8.65015 (s)	8.6266 (s)	8.66296 (d), $J_{13,14}=10.4$	8.65503 (d), $J_{13,14}=11.76$	8.6393 (s)
H14	14.4665 (d), $J_{14,13}=11.4$	14.5164 (s)	14.4126 (s)	14.3699 (d), $J_{14,13}=11.3$	14.475 (d), $J_{14,13}=10.7$	14.489 (s)	14.3654	14.3862 (s)	14.5489 (s)	14.428 (s)	14.4902 (s)	14.1995 (d), $J_{14,13}=10.4$	14.3055 (d) $J_{14,13}=11.76$	14.1835
H15	3.6616 (d), $J_{15,16}=4.6$	3.67599 (s)	3.66358 (d), $J_{15,16}=4.97$	3.64997 (d), $J_{15,16}=5.15$	3.656755 (d), $J_{15,16}=5.18$	3.65104 (d), $J_{15,16}=3.65$	3.6440 (s)	3.6533(s)	3.64558 (d), $J_{15,16}=4.172$	3.6842 (s)	3.6547 (s)	3.65442 (d), $J_{15,16}=4.1$	3.68353 (d), $J_{15,16}=4.75$	3.6633(s)
H16	5.15629 (t), $J_{16,15}=4.6$	5.09196 (s)	5.15744 (s)	5.17728 (t), $J_{16,15}=5.15$	5.15663 (t), $J_{16,15}=5.18$	5.14672 (s)	5.1252 (s)	5.18062 (s)	5.17561 (t) $J_{16,15}=4.172$	5.1236 (s)	5.0587 (s)	5.26849 (s)	5.24188 (t), $J_{16,15}=4.75$	5.2799 (s)
$-CH_2$	–	–	–	–	–	–	–	–	–	–	2.63341 (t), $J=7.686$	–	–	–
$-CH_2$	–	–	–	–	–	–	–	–	–	–	1.58142 (p), $J=7.686$	–	–	–
$-CH_2$	–	–	–	–	–	–	–	–	–	2.6476 (q), $J_{17,18}=7.58$	1.31185 (h), $J=7.686$	–	–	–
$-CH_3$	–	2.61356 (s)	–	–	–	–	–	–	2.3562 (s)	1.1928 (t) $J_{18,17}=7.58$	0.89607 (t), $J=7.686$	–	–	–
$C(=O)CH_3$	–	–	–	–	–	–	–	–	–	–	–	–	–	2.6057 (s)

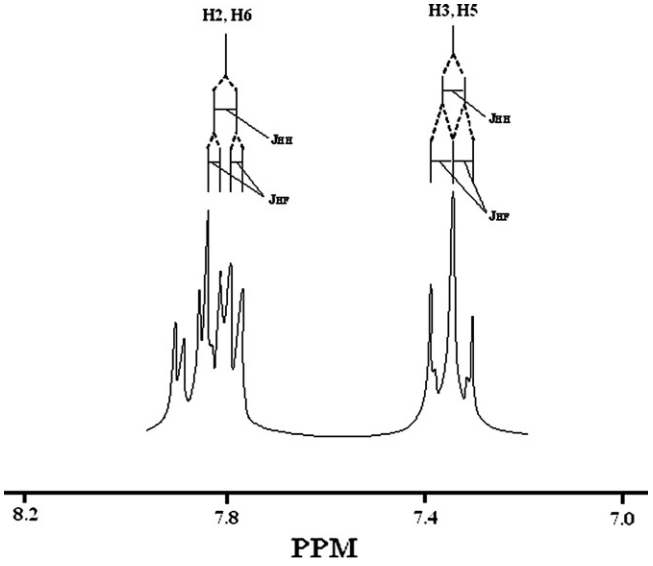

Fig. 9. ^{1}H NMR spectrum of **6e**.

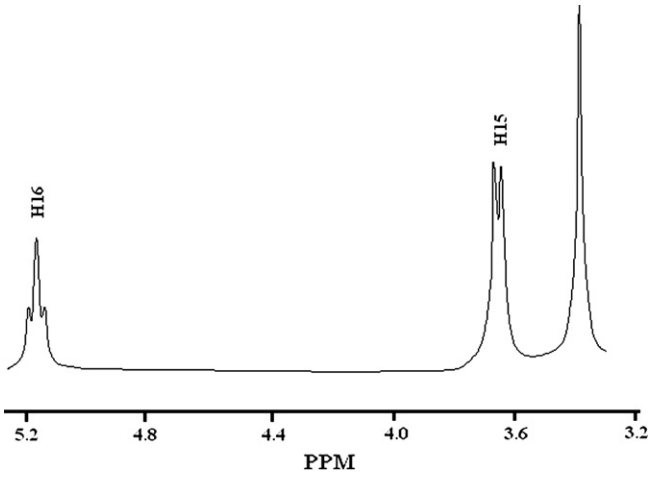

Fig. 10. ^{1}H NMR spectrum of **6e**.

O1, such that a six-membered ring is formed (Fig 13, Table 10). The C13—O1 double bond distance in **4i** is also consistent with the value of the C=O double bond in carbonyl compounds [33]. The C10—O2, —N1=N2—, C—N1 and C7—N2 bond lengths are consistent with values observed in related compounds [28–31].

A view of the molecule of **6a** is shown in Fig 16. The structure of **6a** reveals several points of interest. First, the molecule exists primarily as the keto-amine tautomer in solid state, as indicated by the C10—O1 [1.2913(15) Å], C9-C13 [1.4199(18) Å], C13—N3 [1.2997(16) Å] and C9—C10 [1.4395(18) Å] bond lengths. These bonds are 1.357(2) Å, 1.441(2)Å, 1.285(2) Å and 1.396(2) Å, respectively, in the phenol-imine tautomer (see Scheme below) of 2-(3-methoxysalicylideneamino)-1*H*-benzimidazole [34]. These data show that there is significant

Table 7
^{13}C NMR signals of polyhydroxy azo–azomethine derivates

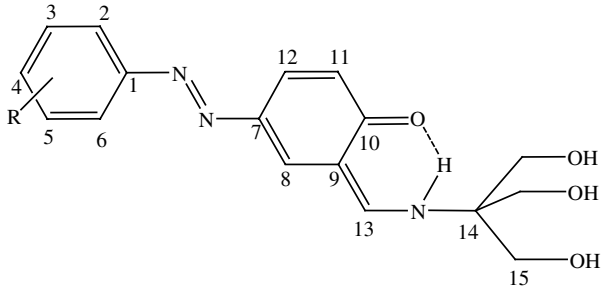

	6a	6b	6c	6d	6e	6f	6g	6h	6i	6j	6k	6l	6m
C1	152.253	150.142	148.263	153.453	148.985 (d), $J_{C1F} = 3.05$	150.998	151.241	151.781	150.313	150.501	150.455	156.125	154.953
C2	121.635	135.956	136.159	121.446	123.626 (d), $J_{C2F} = 8.8$	129.292	123.523	123.669	121.692	121.754	121.630	122.345	121.647
C3	129.100	129.377	127.748	135.943	115.961 (d), $J_{C3F} = 22.7$	123.312	132.127	138.132	129.677	128.421	128.929	124.915	129.388
C4	129.519	130.999	130.670	130.835	162.603 (d), $J_{C4F} = 247.5$	135.275	123.523	95.823	139.590	145.757	144.349	146.894	136.738
C5	129.100	126.447	117.290	128.832	115.961 (d), $J_{C5F} = 22.7$	123.312	132.127	138.132	129.677	128.421	128.929	124.915	129.388
C6	121.635	114.875	130.328	120.058	123.626 (d), $J_{C6F} = 8.8$	129.292	123.523	123.669	121.692	121.754	121.630	122.345	121.647
C7	140.513	141.160	140.692	140.129	140.347	140.377	140.277	140.401	140.685	140.728	140.655	140.429	140.464
C8	134.285	133.968	132.356	133.888	134.325	133.871	135.263	135.288	133.559	133.483	133.441	138.421	136.643
C9	123.130	122.988	123.906	123.719	123.161	123.619	122.445	123.669	122.920	122.841	122.798	124.487	123.968
C10	176.572	176.153	178.038	177.856	176.586	177.445	177.426	177.498	176.007	175.900	175.863	179.490	178.352
C11	114.629	114.680	114.369	114.442	114.611	114.564	114.493	114.577	114.785	114.809	114.759	114.387	114.425
C12	126.357	126.298	126.483	126.306	126.288	126.434	126.350	126.487	126.450	126.457	126.349	126.273	126.320
C13	164.703	164.634	164.892	164.850	164.670	164.645	164.793	164.868	164.679	164.656	164.599	165.215	164.970
C14	65.996	65.999	65.974	65.981	65.985	66.057	65.975	66.074	66.066	66.066	66.009	66.041	65.992
C15	60.559	60.615	60.471	60.490	60.564	60.591	60.511	60.607	60.667	60.684	60.608	60.358	60.452
$-CH_2$	–	–	–	–	–	–	–	–	–	–	34.465	–	–
$-CH_2$	–	–	–	–	–	–	–	–	–	–	32.769	–	–
$-CH_2$	–	–	–	–	–	–	–	–	–	27.889	21.576	–	–
$-CH_3$	–	17.006	–	–	–	–	–	–	20.826	15.214	13.583	–	–
$C(=O)CH_3$	–	–	–	–	–	–	–	–	–	–	–	–	26.683
C=O	–	–	–	–	–	–	–	–	–	–	–	–	181.082

elongation of the C13—N3 bond and contraction of the C10-O1 bond. For quinoid form, these values are quite typical as observed from the *N*,*N*′-di-5-nitrosalicylidene-(*R*,*R*)-1,2-cyclohexanediamine [41], *N*,*N*′-di-5-nitrosalicylidene-(*R*,*S*)-1,2-cyclohexanediamine [42], 6-hydroxy-2-{[tris(hydroxymethyl)methyl]aminomethylene}cyclohexa-3,5-dien-1(2*H*)-one and 6-methoxy-2-{[tris(hydroxymethyl)methyl]aminomethylene}cyclohexa-3,5-dien-1(2*H*)-one [17], *N*-[1,1-bis(hydroxymethyl)-2-hydroxyethyl]salicylaldimine [17,43], *N*-(α-naphthyl)-2-oxy-1-naphthaldimine [44], *N*-(5-chloro-2-hydroxybenzylidene)-4-hydroxyaniline [45], 17α-hydroxy-3-methoxy-16α-[(*E*)-salicylideneamino] estra-1,3,5(10)-triene [46], tris{2-[(3-formyl-5-methyl salicylidene)amino]ethyl}amine [47]. Secondly, the 'hydroxyl' H-atom was located on atom N3, thus confirming a preference for the keto-amine tautomer in the solid state. Finally, there is a strong intramolecular N3—H33···O1 hydrogen bond, which is a common feature of salicylidene systems [35–37]. It has been reported that there may be an orientational disorder in azobenzene, resulting in a shortening of the N=N bond [to 1.189(6) Å] and an elongation of the N—Ph bonds [to 1.473(4) Å]; these bond lengths are 1.249(4) Å and 1.431(4) Å, respectively, in azobenzene with no disorder (Harada et al., 1997). The N1=N2, N1—C1 and N2—C7 bonds in (I) are

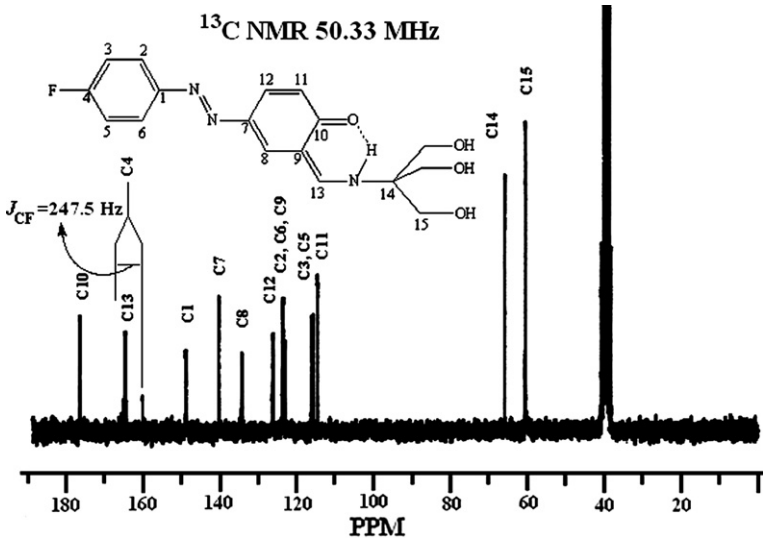

Fig. 11. ^{13}C NMR spectrum of **6e**.

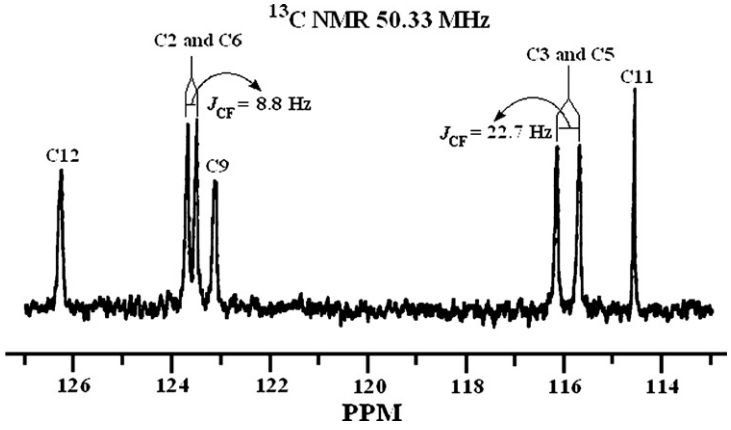

Fig. 12. Part of ^{13}C NMR spectrum of **6e**.

Table 8
Crystal data of **4i** and **6a**

	4i	**6a**
Empirical formula	$C_{11}H_{12}N_2O_2$	$C_{17}H_{19}N_3O_4$
Formula mass	240.26	329.35
Crystal system	Monoclinic	Monoclinic
Space group	*P*21/*c*	*P*21/*c*
a (Å)	21.662(4)	17.570(2)
b (Å)	4.6493(8)	9.6697(12)
c (Å)	11.599(2)	9.3405(11)
β (°)	95.785(4)	92.083(3)
V (Å^3)	1162.3(4)	1585.9(3)
Z	4	4
ρ_{calc} (g cm^{-3})	1.373	1.379
μ (mm^{-1})	0.094	0.100
*R*1/*wR*2 (obsd data: 2σ(*I*)])	0.0570/0.1479	0.0450/0.1089
*R*1/*wR*2 (all data)	0.0840/0.1724	0.0806/0.11273
Goodness of fit	1.102	0.913

Table 9
Selected geometric parameters for **4i** and **6a** (Å,°)

4i		**6a**	
O1—C13	1.219 (3)	O1—C10	1.2913 (15)
O2—C10	1.340 (3)	N1—N2	1.2559 (16)
N1—N2	1.259 (3)	N1—C1	1.4300 (17)
N2—C7	1.425 (3)	N2—C7	1.4157 (17)
N1—C1	1.428 (3)	N3—C13	1.2997 (16)
		C1—C2	1.396 (2)
O2—C10—C11	117.7 (2)	C7—C8	1.3744 (19)
O2—C10—C9	122.7 (2)	C9—C13	1.4199 (18)
C8—C7—N2	117.1 (2)	C9—C10	1.4395 (18)
C12—C7—N2	124.6 (2)	C11—C12	1.3639 (19)
O1—C13—C9	123.7 (2)		
C6—C1—N1	115.2 (2)	N2—N1—C1	113.74 (11)
C2—C1—N1	126.1 (2)	N1—N2—C7	114.34 (11)
		C8—C7—N2	116.37 (12)
C7—N2—N1—C1	179.36 (17)	O1—C10—C9	121.23 (12)
		N3—C13—C9	123.63 (12)
		C1—N1—N2—C7	172.80 (11)

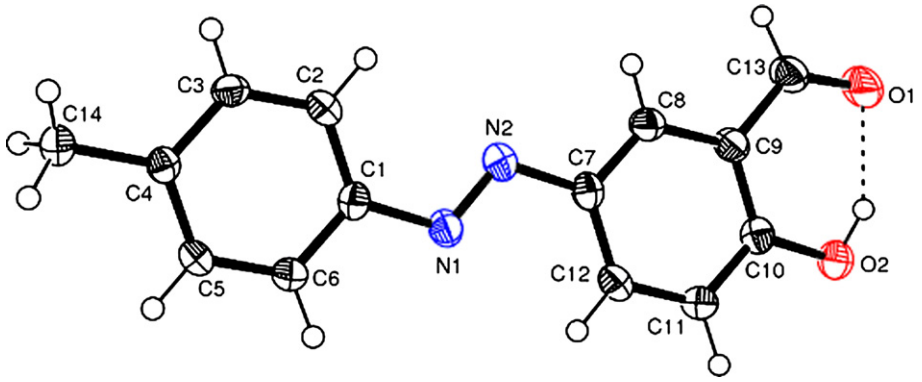

Fig. 13. A view of **4i**, with the atom numbering scheme. Displacement ellipsoids are drawn at the 50% probability level.

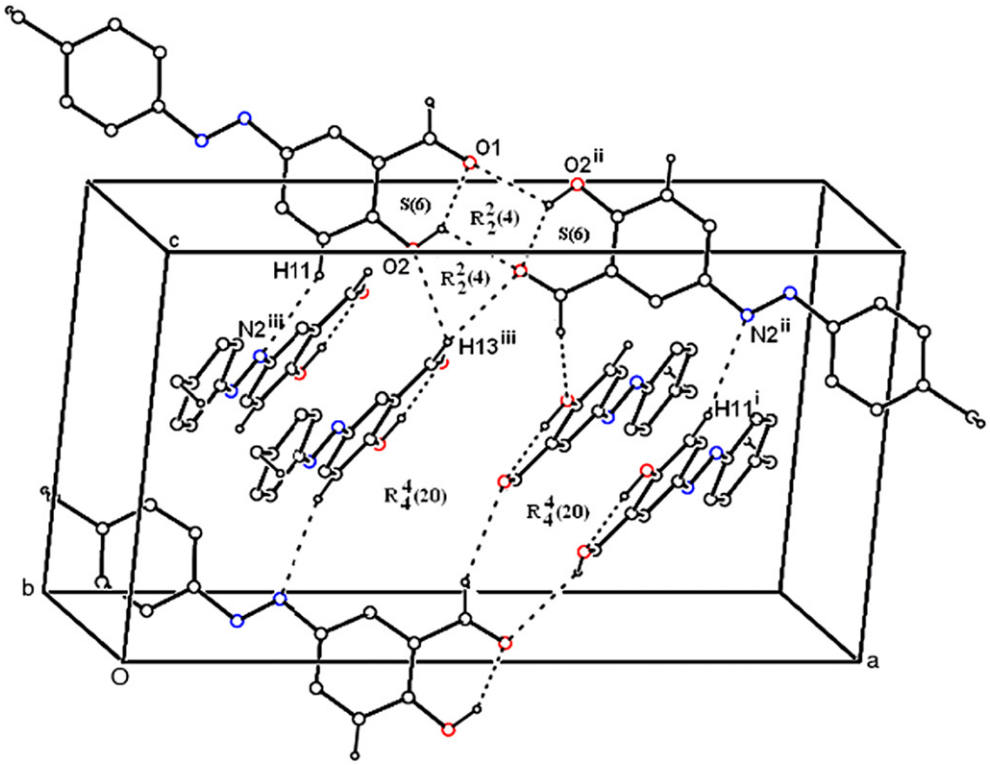

Fig. 14. A partial packing diagram for **4i**, with O—H···O, C—H···O and C—H···N hydrogen bonds shown as dashed lines. the atom numbering scheme. H-atom not involved in these interactions have been omitted. [Symmetry codes: (i) $x, y-1, z-1/2$; (ii) $x, y-1/2, z$; (iii) $x, 1+y, z-1/2$].

1.259(3) Å, 1.428(3) Å and 1.425(3) Å, respectively, indicating that there is no orientational disorder. The two phenyl rings are planar but not coplanar with one another. The dihedral angle between the planes of the phenyl and salicylidene rings is 24.29(4)° and this value is a little larger than those in (*E*)-azobenzenes {(5–15°); [39]} and phenyldiazenylsalicylaldehydes {(3–7°); [28–31]}. Our previous X-ray investigation that the other azo–azomethine compounds of salicylaldehydes have similar dihedral angles and these data are in Table 11. In addition to the intramolecular hydrogen bond, molecules of 6a are linked by intermolecular O—H···O hydrogen bonds into a three-dimensional network (Fig. 17 and Table 10).

2.6. Antimicrobial activity of azo and azomethines

At present study, in vitro potential antimicrobial activity of **4a**, **4c**, **4d**, 4e, **4f**, **4g**, **4i**, **4j**, 4k, **4m** and **6a**, **6c**, **6d**, **6e**, **6f**, **6g**, **6i**, **6j**, **6k** and **7** compounds were tested according to disc diffusion method, are reported in Tables 12 and 13. Antimicrobial activity was measured for 250, 500 and 1000 μg/ml concentrations against Gram-negative bacteria namely *Escherichia coli*, *Salmonella typhimurium*, and *Enterobacter cloaceae*, Gram-positive *Nocardia farcinica*, *Staphylococcus aureus* and *Bacillus subtilis*, yeast *Candida albicans*, and mould *Aspergillus niger*. Streptomycin and ampicillin were used as referance antibiotics for all tests. Among the **4** series compound tested, **4a**, **4d**, **4c**, **4f**, **4e**

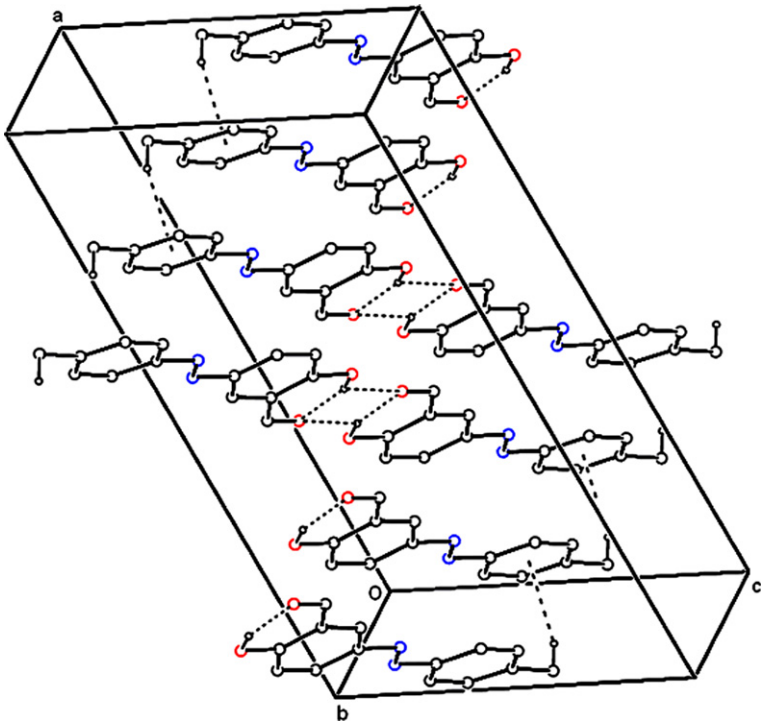

Fig. 15. A partial packing diagram for **4i**, with O—H···O hydrogen bonds and C—H···π interactions shown as dashed lines. the atom numbering scheme. H-atom not involved in these interactions have been omitted.

Table 10
Hydrogen-bonding geometry (Å, °) for **4i** and **6a**

	D–H···A	D–H	H···A	D···A	D–H···A
4i	O2—H1···O1	0.91(4)	1.87(4)	2.679(3)	148(3)
	O2—H1···O1$^{(i)}$	0.91(4)	2.34(4)	2.863(3)	117(3)
	C11—H11···N2$^{(ii)}$	0.97(2)	2.78(2)	3.587(3)	141.10(19)
	C13—H13···O1$^{(iii)}$	0.97(2)	2.84(3)	3.758 (3)	158.70(24)
	C13—H13···O2$^{(iv)}$	0.97(2)	2.64(3)	3.276 (3)	123.21(23)
6a	N3—H1···O1	0.86(2)	1.904(17)	2.616(2)	138.8(15)
	O2—H22···O3i$^{(v)}$	0.84(2)	1.918(19)	2.754(2)	174.0(17)
	O3—H33···O4$^{(v)}$	0.86(2)	1.788(19)	2.630(1)	165.8(19)
	O3—H33···O4$^{(vi)}$	0.94(4)	1.674(18)	2.606(1)	174.0(18)
	C17—H17b···O3$^{(iv)}$	0.97(2)	2.401(15)	3.323(2)	159.5(12)

(i) $1-x,-1-y,-z$.
(ii) $x,-y+1/2,z-1/2$.
(iii) $-x+1,+y+1/2,-z+1/2$.
(iv) $x,-y-1/2,z+1/2$.
(v) $-x,-y,-1-z$.
(vi) $-x,-y,-z$.

and **4j** were found active against only Gram-positive bacteria *S. aureus*, *B. substilis*, and *N. farcinica*. The same compounds were also tested against Gram-negative bacteria, yeast and mould, but there was not any activity detected. However, among these compounds, **4f**, **4m** and **4g** had an effect on Gram-positive *N. farcinica* with the exception of **4k**. In general, all 4 series compound showed weak to moderate antibacterial activity against tested Gram-positive bacteria (Tables 12). Among all 4 series compounds (**4a**–**4m**) the strongest inhibitory effect was observed for **4a** which was derivated from aniline. However, when the substituents were added to phenyl-ring, activity of **4** series compounds were reduced. The greatest inhibitory reduction occurred when **4a** was placed in to para position (compounds **4f**). Reduction range in antimicrobial activity of **4** series compound depending on substituents given as following;

Further studies were conducted to synthesize **6a**, **6c**–**6g**, **6i**–**6k** and compound **7** (Scheme 3) compounds by the addition of **7** to synthesize **6** series compounds. **7** itself did not show an inhibition on tested microorganisms. A detail analysis results reported in Table 13 shows inhibition zones mm in diameter. The comparison of the data obtained for **4a**, **4c**–**4g**, **4i**–**4k** and **4m** and **6a**, **6c**–**6g**, **6i**–**6k** and

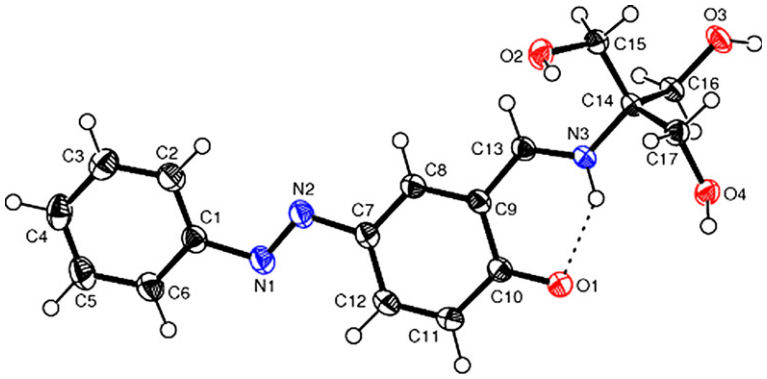

Fig. 16. A view of **6a**, with the atom numbering scheme. Displacement ellipsoids are drawn at the 50% probability level.

Table 11
Some X-ray parameters of some phenyldiazenylsalicylaldehydes (**4**) and trishydroxymethylaminomethane derivatives (**6**)

Compound	Dihedral angle (°)	Intramolecular hydrogen bond		Ref.
		Length (Å)	Angle (°)	
6a	24.29 (4)	2.6158 (15)	38.8 (14)	This paper
4c	4.1(1)	2.962(2)	149(2)	[28]
6c	9.9(1)	2.692(2)	149(2)	[28]
6d	20.47(10)	2.639(2)	139(2)	[18]
4f	3.69(14)	2.702(4)	130(5)	[29]
4g	3.65(16)	2.693(4)	141(5)	[30]
4i	3.65(16)	2.679(3)	148(3)	This paper
4j	6.85(19)	2.615(5)	161(7)	[31]
6j	8.92(2)	2.652(6)	125(6)	[38]

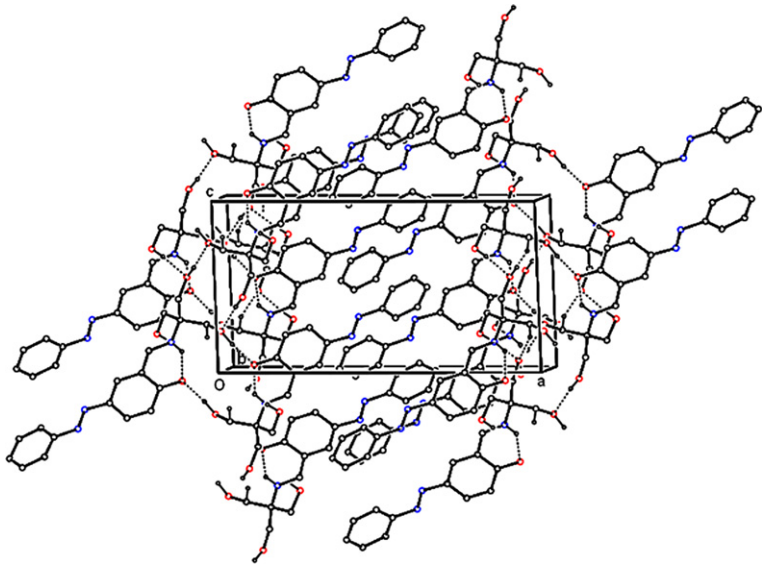

Fig. 17. A partial packing diagram for **6a**, with hydrogen bonds shown as dashed lines. the atom numbering scheme. H-atom not involved in these interactions have been omitted.

compound **7** indicates that the antimicrobial activities of **6** series compounds were markedly increased. All the **6** compounds which found the possess growth inhibitory activity against tested bacteria with the exception of **6g** and **7**. **6** compounds such as **6j**, **6g**, and **6d** showed inhibitory effect on yeast too. On the other hand, while there was no activity **4** series compound with lack of **7**, Some **6** compounds possessed antimicrobial activity such as **6e**, **6a**, **6c** and **6k** were found effective on both yeast and mould by the addition of compound 7.

As can be seen from Tables 12 and 13, **6** compounds had a broad spectrum of action and highest growth inhibitory activity compare to **4** series compounds. The main reason for this increment in **6** compounds action was explored in

Table 12
Observed inhibition zone diameters in millimetres for substrates **4a**, **4c**, **4d**, **4e**, **4f**, **4g**, **4i**, **4j**, **4k** and **4m** and test compounds

Compound	Concentrations (μg)	*S. aureus*	*B. subtilis*	*N. farcinica*	*E. coli*	*S. typhimurium*	*E. cloaceae*	*C. albicans*	*A. niger*
4a	250	10	11	13	–	–	–	–	–
	500	13	12	15	–	–	–	–	–
	1000	16	16	19	–	–	–	–	–
4c	250	12	10[a]	12	–	–	–	–	–
	500	13	11[a]	12	–	–	–	–	–
	1000	15	14[a]	14	–	–	–	–	–
4d	250	9	10[a]	12	–	–	–	–	–
	500	12	12[a]	15	–	–	–	–	–
	1000	14	14[a]	15	–	–	–	–	–
4e	250	8	7	8					
	500	9	7	9					
	1000	12	11	11					
4f	250	–	–	7[a]	–	–	–	–	–
	500	–	–	8[a]	–	–	–	–	–
	1000	–	–	10[a]	–	–	–	–	–
4g	250	–	–	–					
	500	–	–	9					
	1000	–	12	11[a]					
4i	250	8	9	10					
	500	9	11	12					
	1000	10	12	14					
4j	250	9	9	9					
	500	10	10[a]	10					
	1000	11	11	11					
4k	250	–	7	–					
	500	–	8	–					
	1000	–	8	8					
4m	250	–	–	10					
	500	–	–	11					
	1000	–	10	13					
Streptomycin	10	20	17	15	29	16	29	–	–
Ampicillin	10	30	15	–	20	16	20	–	–
DMSO	20 (μl)	–	–	–	–	–	–	–	–

[a] Unclear zone.

terms of whether related to azometin substitution or not. Therefore compound **7** was synthesised and tested on microorganisms. As can be seen from Table 13, compound **7** has no effect on tested microorganism itself. It is thought that the main reason the increasing antimicrobial activity of **6** series compounds which related to presence of azo and azometin groups compounds on the same molecule. The greatest inhibitory activity was shown by **6a** which does not has phenyl-ring. A range of antimicrobial activity of **6** compounds depending on substituents was given as following;

3. Experimental

3.1. Instrumentation

All melting points were analyzed with an electrothermal melting point apparatus. FT-IR spectra were recorded on FTIR-8900 Schmadzu spectrophotometer. Absorption spectra were analyzed on Unicam UV–vis spectrophotometer. The ^{1}H NMR and ^{13}C NMR spectra were taken on Bruker AC 200 MHz spectrometer. Crystal structures were analyzed with STOE STADI 4 diffractometer [40]. Elemental analyses were carried out in TUBITAK Marmara Research Center.

3.2. Dye synthesis and purification

A mixture of 3-chloroaniline (1.275 g, 10 mmol), water (50 ml) and concentrated hydrochloric acid (2.5 ml, 30 mmol) was heated with stirring until a clear solution was obtained. This solution was cooled to 0–5 °C and a solution of sodium nitrite (0.96 g, 14 mmol) in water was added dropwise while the temperature was maintained below 5 °C. The resulting mixture was stirred for 30 min in an ice bath. Salicylaldehyde (1.22 g, 10 mmol) solution (pH 9) was gradually added to a cooled solution of 3-chlorobenzenediazonium chloride, prepared as described above, and the resulting mixture was stirred at 0–5 °C for 60 min

Table 13
Observed inhibition zone diameters in mm for substrates **6a**, **6c**, **6d**, **6e**, **6f**, **6g**, **6i**, **6j**, **6k** and **7** and test compounds

Compound	Concentrations (μg)	*S. aureus*	*B. subtilis*	*N. farcinica*	*E. coli*	*E. cloaceae*	*S. typhimurium*	*C. albicans*	*A. niger*
6a	250	20	23	29	–	–	–	12	9
	500	21	25	32	–	–	–	16	11
	1000	22	27	35	–	–	–	19	12
6c	250	16	18	25	–	–	–	10	8
	500	17	19	28	–	–	–	11	8
	1000	19	20	30	–	–	–	13	9
6d	250	13	16	15	–	–	–	9	–
	500	16	17	19	–	–	–	12	–
	1000	18	18	22	–	–	–	14	–
6e	250	13	13	20	–	–	–	8	8
	500	15	15	21	–	–	–	10	9
	1000	17	18	22	–	–		12	9
6f	250	7	8	9	–	–	–	–	–
	500	9	9	10	–	–	–	–	–
	1000	12	10	13	–	–	–	–	–
6g	250	–	–	7	–	–	–	–	–
	500	–	–	7	–	–	–	–	–
	1000	10	7	7	–	–	–	–	–
6i	250	17	17	15	–	–	–	11	–
	500	18	18	22	–	–	–	13	–
	1000	19	19	24	–	–	–	15	8
6j	250	15	15	15	–	–	–	9	–
	500	16	16	21	–	–	–	12	–
	1000	17	17	23	–	–	–	14	–
6k	250	10	9	9	–	–	–	7	8
	500	11	10	10	–	–	–	7	8
	1000	12	11	13	–	–	–	8	9
7	250	–	–	–	–	–	–	–	–
	500	–	–	–	–	–	–	–	–
	1000	–	–	–	–	–	–	–	–
Streptomycin	10	20	17	15	29	16	29	–	–
Ampicillin	10	9	23	–	20	16	20	–	–
DMSO	20 (μl)	–	–	–	–	–	–	–	–

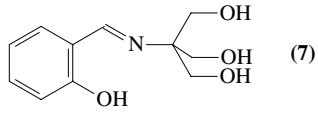

(7)

(E)-2-((1,3-dihydroxy-2-(hydroxymethyl)propan-2-ylimino)methyl)phenol

Scheme 3.

in an ice bath. The product was recrystallized from ethyl alcohol, giving solid 5-(3-chlorophenylazo)salicylaldehyde (mp 127–129 °C). To a solution of this solid (1.302 g, 5 mmol) in butanol (75 ml) was added a solution of tris(hydroxymethyl) aminomethane (0.605 g, 5 mmol) in butanol (25 ml). The mixture was stirred under reflux and water produced in the reaction was distilled out. The resulting orange precipitate was filtered off and recrystallized from ethyl alcohol. Crystals of (I) were obtained after 2 d by slow evaporation from acetonitrile (yield 90%; mp 182–184 °C).

3.3. Antimicrobial activity studies

As a preliminary screening for antimicrobial activity of **6a**, **6c**–**6g**, **6i**–**6k** and **7** and **4a**, **4c**–**4g**, **4i**–**4k** and **4m** were tested against bacterial strains of Gram-positive, *B. subtilis*, *N. farcinica* ATCC 3318, Gram-negative *E. coli* W3110, *Enterobacter cloaceae*, *S. typhimurium* LT2, and, a yeast *Candida albicans* ATCC 10231 *and* a mould *Aspergillus niger*. Antimicrobial studies were performed according to agar disc diffusion method. The following test conditions

were applied; all the compounds were dissolved in dimethylsulfoxide (DMSO, Merck). Nutrient agar (Acumedia) plates were prepared and dried at 35–36 °C for about 30 min in an incubator. Test strains were spreaded on solid nutrient agar surface by using sterile swap. Spreaded inoculum was 3.5×10^5 colony forming unit/ml (0.5 McFarland standard). At the same time, absorbent paper discs were placed on agar surface (5 mm for compounds and 6 mm for antibiotics) and impregnated with known concentrations which determined previously by MIC tests (250, 500 and 1000 μg for each disc). Streptomycin and Ampicillin antibiotics (Bioanalyse) were also used for all test microorganisms as positive control. Blank test showed that DMSO in the preparations of the test solutions does not affect the test organisms. They were inverted and allowed to incubate at 37 °C. The inhibition zone around the disc was calculated edge-to-edge zone of confluent growth, which is usually, corresponds to the sharpest edge of the zone and to be measured diameter in millimetres. All tests were repeated three times and average data taken as final result.

Appendix A. Supplementary data

Supplementary data associated with this article can be found, in the online version, at doi:10.1016/j.molstruc.2006.11.025.

References

[1] S.C. Catino, E. Farris, Concise Encyclopedia of Chemical Technology, John Wiley & Sons, New York, 1985.
[2] K. Venkataraman, The Chemistry of Synthetic Dyes, Academic Press, New York and London, 1970 (Chapter VI).
[3] R. Egli, in: A.P. Peter, H.S. Freeman (Eds.), Colour Chemistry: The Design and Synthesis of Organic Dyes and Pigments, Elsevier, London, 1991 (Chapter VII).
[4] D.M. Marmion, Handbook of U.S. Colorants, third ed., Wiley, New York, 1991, p.23.
[5] H.G. Garg, R.A. Sharma, J. Med. Chem. 12 (1996) 1122.
[6] E.J. Modest, H.N. Schlein, G.E. Foley, J. Pharmacol. 9 (1957) 68.
[7] L.K. Ravindranath, S.R. Ramadas, S.B. Rao, Electrochim. Acta 28 (1983) 601.
[8] Y.-S. Zhou, L.-J. Zhang, X.-R. Zeng, J.J. Vital, X.-Z. You, J. Mol. Struct. 553 (2000) 25.
[9] H. Hard, Organic Chemistry-A Shoert Course, sixth ed., Haughton Mifflin Company, Boston, 1983, p. 313.
[10] E. Hadjoudis, M. Vitterakis, I.M. Maviridis, Tetrahedron 43 (1987) 1345.
[11] X. Xu, X. You, Z. Sun, X. Wang, H. Liu, Acta Crystallogr. C50 (1994) 1169.
[12] T. Iijima, E. Jojima, L. Antonov, St. Stoyanov, T. Stoyanova, Dyes Pigments 37 (1998) 81.
[13] M. Kamel, F. Galil, L. Abdelwahab, A. Osman, J. Prakt. Chem. 313 (1971) 1011.
[14] C.C. Ersanlı, Ç. Albayrak, M. Odabaşoğlu, A. Erdönmez, Acta Crystallogr. E60 (2004) o264.
[15] C.C. Ersanlı, Ç. Albayrak, M. Odabaşoğlu, C. Thöne, A. Erdönmez, Acta Crystallogr. C60 (2004) o133.
[16] M. Odabaşoğlu, Ç. Albayrak, O. Büyükgüngör, Acta Crystallogr. E60 (2004) o142.
[17] M. Odabaşoğlu, Ç. Albayrak, O. Büyükgüngör, P. Lonnecke, Acta Crystallogr. C59 (2003) o616.
[18] M. Odabaşoğlu, Ç. Albayrak, O. Büyükgüngör, H. Goesman, Acta Crystallogr. C59 (2003) o234.
[19] B. Koşar, Ç. Albayrak, M. Odabaşoğlu, O. Büyükgüngör, Acta Crystallogr. E60 (2004) o190.
[20] B. Koşar, Ç. Albayrak, M. Odabaşoğlu, O. Büyükgüngör, Acta Crystallogr. E60 (2004) o246.
[21] K. Ogawa, J. Harada, J. Mol. Struct. 647 (2003) 211.
[22] H. Karaer, PhD Thesis, Ondokuz Mayis University, Samsun, Turkey, 1997, p. 17.
[23] J. Gopal, M. Srinivasan, J. Polym. Sci. Polym. Chem. Ed. 24 (1986) 2789.
[24] St. Stoyanov, L. Antonov, Dyes Pigments 10 (1998) 33.
[25] R.M. Silverstein, F.X. Webster, D.J. Kiemle, Spectrometric Identification of Organic Compounds, seventh ed., 2005, pp. 210 and 323.
[26] L.J. Farrugia, J. Appl. Crystallogr. 30 (1997) 565.
[27] L.J. Farrugia, WinGX, University of Glasgow, Scotland, 1998.
[28] Ç. Albayrak, M. Odabaşoğlu, O. Büyükgüngör, P. Lönnecke, Acta Crystallogr. C60 (2004) o318.
[29] O. Şahin, Ç. Albayrak, M. Odabaşoğlu, O. Büyükgüngör, Acta Crystallogr. E61 (2005) o4149.
[30] O. Şahin, Ç. Albayrak, M. Odabaşoğlu, O. Büyükgüngör, Acta Crystallogr. E61 (2005) o4151.
[31] O. Şahin, Ç. Albayrak, M. Odabaşoğlu, O. Büyükgüngör, Acta Crystallogr. E61 (2005) o4154.
[32] M.C. Etter, Acc. Chem. Res. 23 (1990) 20.
[33] M.G. Loudon, Organic Chemistry, fourth ed., Oxford University press, 2002, p. 837.
[34] M. Odabaşoğlu, Ç. Albayrak, O. Büyükgüngör, Acta Crystallogr. E61 (2005) o425.
[35] A. Filarowski, A. Koll, T. Glowiaka, J. Mol. Struct. 644 (2003) 187.
[36] H. Nazır, M. Yıldız, H. Yılmaz, M.N. Tahir, D. Ülkü, J. Mol. Struct. 524 (2000) 241.
[37] M. Yıldız, Z. Kılıç, T. Hökelek, J. Mol. Struct. 441 (1998) 1.
[38] O. Şahin, Ç. Albayrak, M. Odabaşoğlu, O. Büyükgüngör, Acta Crystallogr. E61 (2005) o2076.
[39] C.J. Brown, Acta Crystallogr. 21 (1966) 146.
[40] Stoe & Cie, STADI 4 and X-RED, Stoe & Cie, Darmstadt, Germany, 1996.
[41] M. Muthuraman, J.-F. Nicoud, R. Masse, G. Desiraju, Z. Kristallogr.-New Cryst. Struct. 216 (2001) 381.
[42] M. Mathuraman, J.-F. Nicoud, R. Masse, G.R. Desiraju, Z. Kristallogr.-New Cryst. Struct. 216 (2001) 383.
[43] G. Asgedom, A. Sreedhara, J. Kivikoski, J. Valkonen, E. Kolehmainen, C.P. Rao, Inorg. Chem. 35 (1996) 5674.
[44] M. Gavranic, B. Kaitner, E. Mestrovic, J. Chem. Crystallogr. 26 (1996) 23.
[45] K. Ogawa, Y. Kasahara, Y. Ohtani, J. Harada, J. Am. Chem. Soc. 120 (1998) 7107.
[46] M. Dubs, R. Krieg, H. Gorls, B. Schonecker, Steroids 65 (2000) 305.
[47] B. Kolodziej, P.M. Dominiak, A. Koscielecka, W. Schilf, E. Grech, K. Wozniak, J. Mol. Struct. 691 (2004) 133.